Novel Aromatic Azo-Containing pH-Sensitive Hydrogels: Synthesis and Characterization

Dong Wang,[†] Karel Dušek,[§] Pavla Kopečková,[†] Miroslava Dušková-Smrčková,[§] and Jindřich Kopeček*[,†,‡]

Department of Pharmaceutics and Pharmaceutical Chemistry/CCCD and Department of Bioengineering, University of Utah, Salt Lake City, Utah 84112, and Institute of Macromolecular Chemistry, Academy of Sciences of the Czech Republic, 16206 Prague 6, Czech Republic

Received May 15, 2002

ABSTRACT: Novel aromatic azo-containing pH-sensitive hydrogels were synthesized by a "one-step" polymer−polymer reaction of two precursors. Precursor **A** was synthesized by copolymerization of a new aromatic azo-containing monomer, *N*-(1-aminohexyl)-4-[[4-(methacryloylamino)phenyl]azo]benzamide (MA-AZO-NH_2), with *N*,*N*-dimethylacrylamide, *N*-*tert*-butylacrylamide, and acrylic acid. Precursor **B** is a copolymer similar to precursor **A** that contains *N*-methacryloylglycylglycine *p*-nitrophenyl ester (MA-GG-ONp) instead of MA-AZO-NH_2. Aromatic azo bonds of MA-AZO-NH_2 in the polymer and in hydrogels were degradable in the presence of fresh rat cecum contents. Control hydrogels were synthesized by cross-linking polymer precursor **B** with a low molecular weight aromatic azo-bond-containing diamine. Modeling of network structure for both novel and control hydrogels was accomplished using a statistical branching theory (theory of branching processes). The theoretical values and experimental data were compared. Conclusions were made for the impact of synthetic mixture compositions and the methods of hydrogel synthesis on the structure of the resulting hydrogel networks.

Introduction

Aromatic azo-containing pH-sensitive hydrogels have been systematically studied and evaluated as colon-specific drug delivery systems.[1−5] Because of the carboxylic acid groups in the network structure, such hydrogels are compact at lower pH but swell as pH value increases. Covered in these hydrogels, fragile therapeutics, such as peptides or proteins, will be protected against digestive enzymes while they are transported through the gastrointestinal (GI) tract. Once inside the colon, where protease activity is much lower than that of small intestine, aromatic azo cross-links in the highly swollen hydrogels will become fully accessible to microbial enzymes and electron mediators. Efficient local release of intact drug may be achieved upon the cleavage of the aromatic azo bonds and dissolution of the hydrogels in the colon. Based on a similar mechanism, linear aromatic azo-containing polymers have been extensively explored as colon-specific drug delivery systems as well.[6,7]

Up to now, three methods had been reported in the synthesis of aromatic azo-containing pH-sensitive hydrogel systems: cross-linking copolymerization,[8] cross-linking of polymer precursors with low molecular weight cross-linking agents, for example, reaction of active ester containing polymer precursors with aromatic azo-containing diamines,[9] and "two-step" polymer−polymer reaction.[10] All of these processes resulted in hydrogels with defects in their three-dimensional network structure.

Theoretically, formation of defects in hydrogel network structure during the gelation procedure depends on a number of factors: initial molar ratios of functional groups, functionality, functionality distribution, degree of polymerization, molecular-weight distributions of the starting components, reactivity of functional groups, changes of functional groups reactivity, and conversion of functional groups during the gelation process. Incomplete conversion may greatly affect the effective cross-linking density (expressed in the terms of concentration of elastically active network chains or EANC), as well as possible entanglements entrapped by cross-linking. During network formation, *intermolecular* reactions may be accompanied by *intramolecular* (cyclization, ring-forming) reactions. Before the gel point, such reactions do not result in the increase of molecular weight. Beyond the gel point, only a fraction of the cyclic paths is considered elastically inactive, that is, not contributing to EANC (and, consequently, to the equilibrium modulus of the network). Such loops are termed *elastically inactive cycles* (EIC). It has been established that the fraction of bonds engaged in EIC is relatively small in the case of cross-linking telechelic polymers by step reactions,[11] whereas it dominates chain cross-linking (co)polymerizations unless large divinyl cross-linkers are used.[12−14]

To prepare novel aromatic azo-containing pH-sensitive hydrogels, *N*-(1-aminohexyl)-4-[[4-(methacryloylamino)phenyl]azo]benzamide (MA-AZO-NH_2) was designed and synthesized in this study. A polymer precursor **A** (with pendent NH_2 groups) was prepared by copolymerization of MA-AZO-NH_2 with *N*,*N*-dimethylacrylamide (DMAA), *N*-*tert*-butylacrylamide (BuAA), and acrylic acid (AA). Precursor **B** was prepared by copolymerization of DMAA, BuAA, AA, and *N*-methacryloylglycylglycine *p*-nitrophenyl ester (MA-GG-ONp). *Novel hydrogels* were synthesized via a "one-step" polymer−polymer reaction between precursors **A**

* To whom correspondence should be addressed. Department of Pharmaceutics and Pharmaceutical Chemistry, University of Utah, 30 S 2000 E Rm. 301, Salt Lake City, UT 84112. Phone: 801-581-4532. Fax: 801-581-3674. E-mail: Jindrich.Kopecek@m.cc.utah.edu.

[†] Department of Pharmaceutics and Pharmaceutical Chemistry/CCCD, University of Utah.

[§] Academy of Sciences of the Czech Republic.

[‡] Department of Bioengineering, University of Utah.

10.1021/ma020745k CCC: $22.00
Published on Web 08/30/2002

and **B**. *Control hydrogels* were synthesized by cross-linking polymer precursor **B** with aromatic azo-containing diamine, *N*,*N*′-(ϵ-aminocaproyl)-4,4′-diaminoazobenzene (NH_2-R-AZO-R-NH_2).[9] The compression moduli of elasticity, content of pendent amino groups, content of aromatic azo groups, and in vitro degradability for both types of hydrogels were then determined. To characterize the relationship between the composition of the cross-linking mixture and the structure of the hydrogels produced, the statistical theory of branching processes (TBP)[11−14] was applied and network parameters for these hydrogels were described. The comparison of experimental data with the theoretical values obtained from the TBP analysis permits the identification of factors responsible for structural defects in the resulting three-dimensional networks studied.

Experimental Section

Abbreviations. The following abbreviations have been used: AA, acrylic acid; AIBN, 2,2′-azobisisobutyronitrile; AZO or azo, diphenyl-diazene; BuAA, *N*-*tert*-butylacrylamide; BV, benzyl viologen; DIPEA, diisopropylethylamine; DCC, dicyclohexylcarbodiimide; DCU, dicyclohexyl urea; DMAA, *N*,*N*-dimethylacrylamide; DMF, *N*,*N*-dimethyl formamide; DMSO, dimethyl sulfoxide; d*n*/d*c*, refractive index increment; EANC, elastically active network chains; FPLC, fast protein liquid chromatography; HOBt, 1-hydroxybenzotriazole; HPMA, *N*-(2-hydroxypropyl)methacrylamide; MA-AZO-NH_2, *N*-(1-aminohexyl)-4-[[4-(methacryloylamino)phenyl]azo]benzamide; MA-AZO-NH_2-Boc, *N*-(*N*-Boc-1-aminohexyl)-4-[[4-(methacryloylamino)phenyl]azo]benzamide; MA-GG-ONp, *N*-methacryloylglycylglycine *p*-nitrophenyl ester; MM, methyl morpholine; M_n, number-average molecular weight; MPA, mercaptopropionic acid; M_w, weight-average molecular weight; MWD, molecular weight distribution; NH_2-R-AZO-R-NH_2, *N*,*N*′-(ω-aminocaproyl)-4,4′-diaminoazobenzene; pgf, probability generating functions; poly(HPMA-*co*-MA-AZO-NH_2), poly{*N*-(2-hydroxypropyl)methacrylamide-*co*-*N*-(1-aminohexyl)-4-[[4-(methacryloylamino)phenyl]azo]benzamide}; SEC, size exclusion chromatography; TBP, theory of branching processes; TFA, trifluoroacetic acid; THF, tetrahydrofuran.

Materials. Chemicals: 4-(4-Aminophenylazo)benzoic acid hydrochloride,[15] NH_2-R-AZO-R-NH_2,[9] HPMA,[16] and MA-GG-ONp[17] were synthesized as described previously. If not specified, all reagents and solvents were purchased from Aldrich (Milwaukee, WI) or Sigma (St. Louis, MO). Acrylic acid and *N*,*N*-dimethylacrylamide were distilled under reduced pressure. *N*-*tert*-butylacrylamide was recrystallized from acetone.

In Vitro Degradation Medium: Sprague−Dawley rats were sacrificed with iv injection of pentobarbital overdose.[18] Cecum contents were removed and stirred in 0.1 M phosphate buffer to make a 10 wt % suspension. The aliquots were bubbled with N_2 and stored at −20 °C. This procedure was a part of the animal protocol (00-09008) being approved by the Institutional Animal Care and Use Committee (IACUC) of University of Utah and was strictly observed.

Methods. All polymers were characterized by SEC using ÄKTA FPLC (Amersham Pharmacia Biotech) equipped with UV, refractive index (RI), and laser light scattering (MINI DAWN, Wyatt Technology, Santa Barbara) detectors. SEC measurements were carried out on Superose 6 columns (analytical) with phosphate-buffered saline, PBS (pH = 7.3), as the eluent. The average molecular weights of the polymers were calculated with ASTRA chromatography software (Wyatt Technology) on the basis of laser light scattering data. The d*n*/d*c* of each of the polymers was determined in the same buffer on an OPTILAB DSP interferometric refractometer (Wyatt Technology).

^{1}H NMR spectra were recorded on a Varian Unity 500 MHz NMR spectrometer. The solvent peak was used as reference (d_6-DMSO, 2.49 ppm).

UV spectra were obtained on a CARY 400 Bio UV−visible spectrophotometer (Varian Analytical Instruments, Walnut Creek, CA).

Synthesis of 4-(4-Methacryloylaminophenylazo)benzoic acid. Briefly,[19] 4-(4-aminophenylazo)benzoic acid hydrochloride (1.9 g, 6.8 mmol) and diisopropylethylamine (2.5 mL, 14.4 mmol) were dissolved in THF (150 mL). Methacryloyl chloride (0.67 mL, 6.8 mmol, in 20 mL of methylene chloride) was added dropwise with stirring at −5 °C. The mixture was stirred overnight at room temperature. HCl (5.0 mL, 6 N) was added to neutralize excess diisopropylethylamine. The solvent was removed under vacuum. The resulting solid was washed with water, dissolved in THF, and dried over Na_2SO_4. THF was removed and the remaining solid was recrystallized twice to obtain a deep red powder product. The yield was 0.95 g (44%). ESI ($C_{17}H_{15}N_3O_3$, fw = 309.11): 310.2 (M + 1). ^{1}H NMR (DMSO-d_6): d = 1.97 ppm (s, CH_3); 5.59 and 5.86 ppm (d, CH_2); 7.92−8.13 ppm (m, C_6H_4−N=N−C_6H_4); 10.16 ppm (s, CONH); 13.18 ppm (br s, COOH).

Synthesis of *N*-(*N*-Boc-1-aminohexyl)-4-[[4-(methacryloylamino)phenyl]azo]benzamide (MA-AZO-NH_2-Boc). 4-(4-Methacryloylaminophenylazo)benzoic acid (0.45 g, 1.455 mmol), *N*-Boc-1,6-diamino hexane hydrochloride (0.763 g, 2.91 mmol), diisopropylethylamine (0.5 mL, 2.91 mmol), and HOBt (0.393 g, 2.91 mmol) were suspended in methylene chloride (20 mL) and cooled to −5 °C. DCC (0.6 g, 2.91 mmol) was dissolved in methylene chloride (1.5 mL) and slowly added to the mixture. The suspension was stirred overnight at 4 °C and for 2 h at room temperature. The solid was filtered, washed with methylene chloride, and suspended in DMF (20 mL). The suspension was kept at 4 °C for 3 days. The needlelike crystals (DCU) were then filtered off. The filtrate was dried by oil pump. Diethyl ether was added, and the solid product was filtered off and dried under vacuum. Dry product was suspended in cyclohexane and stirred overnight; the nonsoluble portion was filtered, washed with diethyl ether, and dried. This purification process was repeated once. The yield was 0.29 g (39%). ESI ($C_{28}H_{37}N_5O_4$, fw = 507.28): 508.3 (M + 1), 408.1 (M − Boc + 1, formic acid used in ESI procedure). ^{1}H NMR (DMSO-d_6): d = 1.25−1.54 ppm [m, $(CH_3)_3$ and CH_2−$(CH_2)_4$−CH_2]; 1.97 ppm (s, CH_3); 2.90 ppm (m, CH_2NHCOO); 3.26 ppm (m, CH_2NHCO); 5.59 and 5.86 ppm (d, CH_2); 6.77 ppm (s, NHCOO); 7.92−8.13 ppm (m, C_6H_4−N=N−C_6H_4); 8.59 ppm (s, C_6H_4−CONH); 10.16 ppm (s, CONH−C_6H_4).

Synthesis of *N*-(1-Aminohexyl)-4-[[4-(methacryloylamino)phenyl]azo]benzamide (MA-AZO-NH_2). *N*-(*N*-Boc-1,6-diaminohexyl)-4-[[4-(methacryloylamino)phenyl]azo]benzamide (100 mg) was dissolved in TFA (10 mL) and stirred at room temperature for 2 h. The solution was dried and redissolved in DMSO. It was directly used for the synthesis of hydrogel precursors **A**. The peak assigned to Boc disappeared in the ^{1}H NMR spectrum after deprotection.

In Vitro Degradability of MA-AZO-NH_2. MA-AZO-NH_2 was copolymerized with *N*-(2-hydroxypropyl)methacrylamide (HPMA) to obtain poly(HPMA-*co*-MA-AZO-NH_2) ([azo] = 3.29×10^{-4} mol/g). In vitro degradability of the MA-AZO-NH_2 side chains of the water-soluble copolymer was evaluated chemically and biologically.

To the aqueous solution of poly(HPMA-*co*-MA-AZO-NH_2) (1 mL; [azo] = 1.65 mM; in phosphate buffer, pH = 7.4), sodium hydrosulfite solution (0.5 mL; 0.2 M; in PBS, pH = 7.4) was added. The mixture was vortexed, and the disappearance of the aromatic azo absorbance (demonstrating the cleavage of azo bond) was monitored.

Fresh rat cecum content suspension (4.5 mL, 10 wt % in 0.1 M phosphate buffer) was mixed with α-D-glucose (0.9 mL, 150 mg/mL in 0.1 M phosphate buffer) in a vial (20 mL). The mixture was bubbled with N_2 for 5 min, and then the vial was sealed. The suspension was incubated at 37 °C for 14 h. Poly(HPMA-*co*-MA-AZO-NH_2) stock solution (0.9 mL, 3.75 mg/mL in 0.1 M phosphate buffer) or methyl orange stock solution (5×10^{-4} M in 0.1 M phosphate buffer) were added into the preincubated suspension with phosphate buffer (2.7 mL, 0.1 M). The suspension was then bubbled with N_2 for 5 min and

incubated at 37 °C. At selected time intervals, suspensions (0.7 mL) were withdrawn and acidified with HCl (0.05 mL, 1 M). These were centrifuged at 4 °C, and the UV absorption of supernatant was measured at 350 nm [poly(HPMA-*co*-MA-AZO-NH_2)] or 530 nm (methyl orange).[19]

Synthesis of Precursor A. Precursor **A** was synthesized by free radical copolymerization of MA-AZO-NH_2 with other comonomers. A typical synthesis procedure is as follows: *N*-*tert*-Butyl acrylamide (BuAA) (0.1272 g, 0.001 mol, 10 mol %), *N*,*N*-dimethylacrylamide (DMAA) (0.436 g, 0.0044 mol, 44 mol %), acrylic acid (AA) (0.288 g, 0.004 mol, 40 mol %), MA-AZO-NH_2 (0.245 g, 0.0006 mol, 6 mol %,), 2,2′-azobisisobutyronitrile (AIBN; initiator) (0.05 g, 0.0003 mol), and mercaptopropionic acid (MPA; chain transfer agent) (0.0679 mmol) were dissolved in DMSO (10 mL), bubbled with N_2 for 5 min, and sealed in an ampule. The reaction mixture was polymerized at 50 °C for 24 h, and the copolymer was isolated by precipitation into diethyl ether. The resulting sticky product was redissolved in MeOH and precipitated into acetone/diethyl ether = 1/1. The yield of copolymer was 350 mg (65%). The content of aromatic azo groups was determined by UV spectrophotometry at 371 nm (ϵ_{371nm} = 19 600, DMSO).

Synthesis of Precursor B. Precursor **B** was synthesized by a free radical copolymerization of MA-GG-ONp with the other comonomers. Typically, BuAA (0.2544 g, 0.002 mol, 10 mol %), DMAA (0.8723 g, 0.0088 mol, 44 mol %), AA (0.5765 g, 0.008 mol, 40 mol %), MA-GG-ONp (0.3856 g, 0.0012 mol, 6 mol %), AIBN (0.1 g, 0.000 61 mol), and MPA (0.1358 mmol) were dissolved in DMSO (20 mL). The ampule was purged with N_2 for 5 min and then sealed. It was polymerized at 50 °C for 24 h. The polymer solution was then precipitated into diethyl ether/acetone (1/1 v/v). The copolymer was dissolved in MeOH and reprecipitated into diethyl ether/acetone (1/1 v/v). The yield of polymer was 750 mg (68.5%).

Synthesis of Novel Hydrogels by Polymer−Polymer Reaction. The protocol for a typical hydrogels synthesis by polymer−polymer reaction is as follows: Precursor **A** (110 mg, $[NH_2] = 3.56 \times 10^{-5}$ mol) was dissolved in DMSO (0.6 mL). Precursor **B** (290 mg, $[ONp] = 3.56 \times 10^{-5}$ mol) was dissolved in DMSO (1.7 mL). TFA solution (in DMSO, 50 μL, containing 7.13×10^{-5} mol of TFA) was added to precursor **A**, and the solutions were well mixed. The resulting solution was mixed with precursor **B** solution, and the mixture was vortexed for 1 min. Methyl morpholine (MM) solution (in DMSO, 50 μL, containing 1.462×10^{-4} mol of MM) was added into the resulting solution, and the mixture was vortexed for 1 min. It was quickly transferred into a mold. Gelation point was typically reached after 1 h. Twenty-four hours later, the gel disks were removed from the mold and immerged in DMSO/EtOH/HCl (0.01 M) = 1/1/1 for 2 days, followed by one week in EtOH for elimination of unreacted compounds.

Synthesis of Control Hydrogel by Cross-Linking of Precursor B with *N*,*N*′-(ω-aminocaproyl)-4,4′−diaminoazobenzene (NH_2-R-AZO-R-NH_2). Similar to a protocol described previously,[9] NH_2-R-AZO-R-NH_2 was mixed with TFA in DMSO. This solution was added to precursor **B**, and the solutions were well mixed. This was followed by addition of methyl morpholine (MM). The resulting solution was then quickly transferred into a mold. The gelation point was reached after about 1 h. The gels were then purified as described above.

Determination of Nonreacted Pendent Amino Groups in Hydrogels. The amount of nonreacted amino groups in the hydrogels was determined spectroscopically using the ninhydrin method.[20] Briefly, the dry hydrogel was ground into tiny particles and soaked in acetate buffer (4 N, pH = 5.5, 0.5 mL) for 1 h. The content of NH_2 in the hydrogels was determined from the supernatant solution by ninhydrin assay with glycine as the standard.[9]

Determination of the Content of Aromatic Azo Bonds in the Hydrogels. The amount of aromatic azo bonds in the hydrogels was determined spectrophotometrically.[9] Briefly, dry hydrogel (about 5 mg) was ground and suspended in NaOH (2 N, 5 mL). The suspension was incubated at 37 °C for 4 days to dissolve the hydrogel. The resulting solution was either diluted 10 or 20 times with deionized (DI) water (hydrogels synthesized by one-step polymer−polymer reaction, $\epsilon_{360\ nm}$ = 24 200, in 0.1 or 0.2 N NaOH) or diluted with an equal amount of DMSO and further diluted with DMSO/2 N NaOH (1/1) [hydrogels synthesized with NH_2-R-AZO-R-NH_2, $\epsilon_{445\ nm}$ = 23 000, in DMSO/2 N NaOH (1/1)]. The content of aromatic azo bonds in hydrogels was determined by their UV spectra.

Degradation of Hydrogels in Vitro. Fresh rat cecum content (described above, 9 mL), α-D-glucose (50 mg/mL, 1 mL, in 0.1 M phosphate buffer), phosphate buffer (0.1 M, 9 mL), and benzyl viologen (20 mg/mL, 1 mL, in 0.1 M phosphate buffer) were mixed together and bubbled with N_2 for 10 min. The container was closed tightly and sealed. The mixture was incubated at 37 °C for 15 h. The hydrogel disk was then immersed in the suspension. The mixture was bubbled with N_2 again, sealed, and incubated at 37 °C. At chosen time intervals, the hydrogel disk was retrieved and washed with EtOH/H_2O = 1/1. The gel was then transferred into 0.1 M phosphate buffer. After its wet weight was measured, it was immersed into DI water and later into ethanol. Later, the gel was dried under reduced pressure in the presence of P_2O_5. Changes in aromatic azo bonds content and the weight of the hydrogels were determined to evaluate the degradation process.

Characterization of the Mechanical Properties of the Hydrogels. Moduli of elasticity of the hydrogels in compression were determined using a bench comparator (B. C. Ames Co. Waltham, MA) as described previously.[21] Briefly, all gels were preincubated in phosphate buffer (0.1 M, pH = 7.4) at 37 °C for 2 days before the measurement. After application of a given force, the equilibrium height of the gel was measured. The force was removed, and the gel was allowed to relax to its original height (confirmed by measuring original height each time). Then, a new force was applied. The maximum deformation was limited to within 20% of its original height. Five to nine different values of force and corresponding heights were obtained for each gel, and the modulus was calculated as the average of three measurements. The equilibrium modulus of the swollen sample, $(G_e)_{sw}$ was calculated from the following equation:[22]

$$\frac{F}{A} = -(G_e)_{sw}(\lambda - \lambda^{-2}) \tag{1}$$

where F is the force applied onto the gel surface, A is the surface area of the swollen gel, l and l_0 are the heights of the gel after and before weight is applied, and λ is the gel deformation where $l = \lambda l_0$.

Using the junction-fluctuation rubber elasticity theory of Flory,[23] we can calculate the concentration of elastically active network chains (EANC), ν_e, from $(G_e)_{sw}$ using the equation

$$(G_e)_{sw} = ART\nu_e\phi_2^{1/3}(\phi_2^o)^{2/3} \tag{2}$$

where R is the gas constant, T is the absolute temperature, ϕ_2 is the volume fraction of the polymer in the swollen gel, and ϕ_2^o is the volume fraction of polymer at network formation; $1 - \phi_2^o$ is the volume fraction of the diluent. If soluble fraction (sol) is present at the end of network formation, it also should be considered as diluent. The concentration of EANC, ν_e, is related to unit dry volume of the network. A is the front factor, which, within the Flory junction-fluctuation theory, varies between $A_{ph} = (f_e - 2)/f_e$ (phantom network) and $A_{aff} = 1$ (affine network), where f_e is the number-average functionality of an elastically active cross-link; in our case, $f_e = 3$. A is close to A_{ph} for large-strain tensile moduli and swollen systems and close to A_{aff} for small strain moduli, compression modes and unswollen systems. Because of the small-strain compression measurements used in this work, we have assumed $A = A_{aff} = 1$. The validity of this assumption is corroborated by the observation that the reduced values of $(F/A)/(\lambda - \lambda^{-2})$ do not depend on deformation.

The value of ϕ_2^o and ϕ_2 could be easily obtained from the following equations:[9]

$$\phi_2^o = \frac{\frac{w_p}{d_p}}{\frac{w_p}{d_p} + \frac{w_{DMSO}}{d_{DMSO}}} \quad (3)$$

$$\phi_2 = \frac{\frac{w_p}{d_p}}{\frac{w_p}{d_p} + \frac{w_{H_2O}}{d_{H_2O}}} \quad (4)$$

where w_p and d_p refer to the weight and density of hydrogel precursors (polymer), w_{DMSO} and d_{DMSO} refer to the weight and density of DMSO, and w_{H_2O} and d_{H_2O} refer to the weight and density of water.

Calculation of Parameters Characterizing Network Structure of Hydrogels

Formation of both types of hydrogels is based on bond formation by a stepwise reaction of functional groups A and B, A + B → AB. In the case of the aromatic azo-containing *novel hydrogels* synthesized by "one-step" polymer−polymer reaction, the A (amino groups) and B (ONp active ester) groups are parts of precursor **A** and precursor **B**, respectively (for the convenience in the discussion below, molecules containing A groups or amino groups are termed as component **A**, molecules containing B groups or ONp ester groups are termed as component **B**). In the case of *control hydrogels* synthesized by cross-linking reaction of active ester-containing polymer precursor **B** with aromatic azo-containing diamines, the diamine (component **A**) bears two A groups (amino groups) and the component **B** is polymer precursor **B** (bearing ONp active ester groups) as in the case of *novel hydrogels*.

The development of the network structure is described theoretically by the statistical theory of branching processes (TBP) based on generation of structures by assemblage of component units in different reaction states. The reaction states differ in the number and type of reacted functional groups and bonds in which these reacted groups are engaged. The formalism of probability generating functions and cascade substitution were used as tools. Several assumptions have been used in the derivation given below: (1) All functional groups A and all functional groups B have the same reactivity that is independent of conversion. (2) The copolymers composed of monomer units carrying A and B groups and other monomer units without functional groups have the most probable distribution of degrees of polymerization.[24] (3) The distributions of units carrying A and B groups and nonfunctional units within copolymer chains are random and are described by polynomial (binomial) expansion. (4) Intramolecular reactions are not considered. Beyond the gel point, uncorrelated circuit closing is allowed.

Network structures generated with TBP range from finite, soluble molecules to "infinite" gel and its substructures such as elastically active network chain or dangling chains. In the models described below, the building units are equivalent with component units A and B.

System 1−Novel Hydrogel by "One-Step" Polymer−Polymer Reaction. The following quantities characterize the components **A** and **B** and the progress of the cross-linking reaction: P_{An} and P_{Bn} are the number-average degrees of polymerization of components **A** and **B**, respectively; x_A and x_B are molar fractions of units A and B, respectively, in components **A** and **B**; M_A, M_B, and M_i are the molecular weight of monomer units A, B, and i, respectively; M_{An} and M_{Bn} are the number-average molecular weight of a monomer unit in polymer precursors **A** and **B**, respectively; r_A is the initial molar ratio of groups A to B; ρ is the specific gravity of the dry network [mass/volume]; α_A and α_B are the molar conversions of A and B groups, respectively ($\alpha_A r_A = \alpha_B$). From this basic information, other quantities were derived, such as the following: q_A and q_B are parameters of the degree of polymerization distribution ($q_A = P_{An}/(P_{An} - 1)$, $q_B = P_{Bn}/(P_{Bn} - 1)$); n_A and n_B are molar fractions of polymer precursors (components) **A** and **B**, respectively ($n_A = P_{Bn}x_B r_A/(P_{An}x_A + P_{Bn}x_B r_A)$, $n_B = 1 - n_A$); m_{XA} and m_{XB} are weight fractions of monomer units A in the polymer precursor **A** and monomer units B in the polymer precursor **B**, respectively ($m_{XA} = x_A M_A/(x_A M_A + \sum x_i M_i)$, $m_{XB} = 1 - m_{XA}$, where x_i and M_i are molar fractions and molecular weights of other comonomer units); M_{0n} is the number-average molecular weight of component unit ($M_{0n} = n_A P_{An} M_A + n_B P_{Bn} M_B$.

The components **A** and **B** in the *novel hydrogels* (by "one-step" polymer−polymer reaction) and component **B** in the *control hydrogels* (synthesized via reaction of active ester containing polymer precursors **B** with aromatic azo-containing diamines) are polydisperse in degree of polymerization, as well as in composition. Because the most probable distribution[24] is assumed, the generating function for this number-fraction distribution reads

$$N(Z) = \frac{(1-q)Z}{1-qZ} = \sum_{j=1}^{\infty}(1-q)q^{j-1}Z^j \quad (5)$$

In eq 5, $q = 1 - 1/P_n$, and the coefficient at Z^j equal to $(1-q)q^{j-1}$ is the number fraction of the j-mer.[24] In the case of a binary copolymer of A and X monomer units, the compositional distribution is assumed to be random, that is, for the j-mer, the corresponding number-fraction distribution function $C_j(Z_A,Z_X)$ reads

$$C_j(Z_A,Z_X) = (x_A Z_A + x_X Z_X)^j = \sum_{k=0}^{j}\binom{j}{k}x_A^{j-k}x_X^k Z_A^{j-k}Z_X^k \quad (6)$$

Here, the coefficient at $Z_A^{j-k}Z_X^k$ is the number fraction of j-mer composed of $j - k$ monomer units A and k monomer units X. The compositional distribution extending over the degree of polymerization distribution, which is relevant for analysis of cross-linking, is obtained by substitution of Z in eq 6 by $(x_A Z_A + x_X Z_X)$, ($x_A + x_X = 1$), and

$$N(Z) \rightarrow N(Z_A,Z_X)$$

and

$$Z \rightarrow (x_A Z_A + x_X Z_X)$$

The pgf characterizing the cross-linking system in terms of the number of bonds issuing from component units (copolymer chains) **A** and **B** occurring in different

reaction states is described by the following equation:

$$F_{0n}(z_A,z_B) = n_A\frac{(1-q_A)\zeta_A(z_B)}{1-q_A\zeta_A(z_B)} + n_B\frac{(1-q_B)\zeta_B(z_A)}{(1-q_B\zeta_B(z_A))} \quad (7)$$

where

$$\zeta_A(z_B) = 1 - x_A + x_A(1-\alpha_A+\alpha_A z_B)$$

and

$$\zeta_B(z_A) = 1 - x_B + x_B(1-\alpha_B+\alpha_B z_A)$$

where z_A and z_B are variables of the pgf characterizing the oriented bonds B → A and A → B, respectively. For instance, the coefficient at z_B^i is equal to the population (number or molar fraction) of the **A**-copolymer component units extending i bonds A → B to **B**-copolymer units. This pgf is a number-fraction generating function. The pgf for the number of additional bonds issuing from units already bonded by one of their reacted functional groups, $F_A(z_B)$ and $F_B(z_A)$ are obtained in a standard way by differentiation of the pgf F_{0n}

$$F_A(z_B) = \frac{\partial F_{0n}(z_A,z_B)}{\partial z_B}\aleph_A = \frac{(1-q_A)^2}{(1-q_A\zeta_A(z_B))^2} \quad (8)$$

where

$$\aleph_A = \left(\frac{\partial F_{0n}(z_A,z_B)}{\partial z_B}\right)^{-1}_{z_B=1}$$

Likewise,

$$F_B(z_A) = \frac{\partial F_{0n}(z_A,z_B)}{\partial z_A}\aleph_B = \frac{(1-q_B)^2}{(1-q_B\zeta_B(z_A))^2} \quad (9)$$

The gel-point is given by the condition, valid for alternating systems,[11,12] that the product of values of derivatives of $F_A(z_B)$ and $F_B(z_A)$with respect to z_B and z_A, respectively, $F'_A(1)$ and $F'_B(1)$ (in which $z_A = z_B = 1$),

$$F'_A(1)F'_B(1) = \frac{4q_Aq_Bx_Ax_B\alpha_A\alpha_B}{(1-q_A)(1-q_B)} \quad (10)$$

is equal to 1.

The explicit equation for the gel-point conversion reads

$$(\alpha_A)_{crit} = (\alpha_B)_{crit}/r_A = \left(\frac{4q_Aq_Bx_Ax_Br_A}{(1-q_A)(1-q_B)}\right)^{-1/2} \quad (11)$$

Beyond the gel point, the bonds issuing from copolymer chains (component units) can have finite or infinite continuation. The quantity determining whether a bond has finite or infinite continuation is the extinction probability. The quantity v_A is the conditional probability that, given a bond B → A exists, it issues only a finite sequence of bonds looking out of the unit. The extinction probability v_B has a similar significance for the bond A → B. The extinction probabilities v_A and v_B are defined by the relations

$$v_A = F_A(z_B{=}v_B) = \frac{(1-q_A)^2}{(1-q_A\zeta_{Av})^2} \quad (12)$$

$$v_B = F_B(z_A{=}v_A) = \frac{(1-q_B)^2}{(1-q_B\zeta_{Bv})^2} \quad (13)$$

where

$$\zeta_{Av} = 1 - x_A + x_A(1-\alpha_A+\alpha_A v_B)$$

and

$$\zeta_{Bv} = 1 - x_B + x_B(1-\alpha_B+\alpha_B v_A)$$

The values of v_A and v_B are obtained by numerical solution of eqs 12 and 13 looking for the root in the interval (0,1).

The soluble fraction (sol) is composed of component units (copolymer chains) that have no bond with infinite continuation. These units contribute by their weight. It can be shown that the weight-fraction distribution for the component **A**, $W_A(Z_X,Z_A)$, can be obtained by differentiation of the number-fraction generating function

$$N_A(Z_X,Z_A) = \frac{(1-q_A)\theta}{(1-q_A\theta)}$$

where

$$\theta = (x_X Z_X^{M_X} + x_A Z_A^{M_A})$$

Therefore

$$W_A(Z_X,Z_A) = \frac{(1-q_A)^2}{(1-q_A\theta)^2}\theta_w \quad (14)$$

where

$$\theta_W = m_{XX}Z_A^{M_A} + m_{XA}Z_A^{M_A}$$

and

$$m_{XX} = 1 - m_{XA}$$

The contribution to the soluble fraction by component **A** is thus equal to

$$[W_A(Z_X,(1-\alpha_A+\alpha_A v_B)Z_A)]_{Z_A=Z_X=1}$$

The soluble fraction w_s is then given by

$$w_s = m_A\frac{(1-q_A)^2\zeta_{Aw}}{(1-q_A\zeta_{Av})^2} + m_B\frac{(1-q_B)^2\zeta_{Bw}}{(1-q_B\zeta_{Bv})^2} \quad (15)$$

where

$$\zeta_{Aw} = 1 - m_{XA} + m_{XA}(1-\alpha_A+\alpha_A v_B)$$

$$\zeta_{Bw} = 1 - m_{XB} + m_{XB}(1-\alpha_B+\alpha_B v_A)$$

The weight fraction of gel w_g is equal to

$$w_g = 1 - w_s \tag{16}$$

Elastically active network chains (EANC) are sequences of units between elastically active cross-links (branch points) (EAC). An EAC is a branch point from which 3 or more bonds issue to infinity. The number of EANC is routinely derived from the number of bonds with infinite continuation issuing from EAC.

The pgf counting bonds with infinite continuation issuing from component units, $T(z)$, is constructed in such a way that the probability that a bond exists, given by α_A or α_B, is weighted by the probability, $1 - v_B$ or $1 - v_A$, that it has an infinite continuation:

$$T(z) = n_A\frac{(1 - q_A)\xi_A(z)}{(1 - q_A\xi_A(z))} + n_B\frac{(1 - q_B)\xi_B(z)}{(1 - q_B\xi_B(z))} = \sum_{i=0}^{\infty} t_i z^i \tag{17}$$

where

$$\xi_A(z) = 1 - x_A + x_A(1 - \alpha_A + \alpha_A(v_B + (1 - v_B)z))$$

$$\xi_B(z) = 1 - x_B + x_B(1 - \alpha_B + \alpha_B(v_A + (1 - v_A)z))$$

The coefficient t_i is equal to the molar fraction of component units **A** and **B** having i monomer units with reacted groups that extend bonds with infinite continuation. Such unit is called active and also represents a branch point. An active unit may become an elastically active branch point, if it satisfies the condition that it issues at least three paths with infinite continuation. Then it contributes to the number of EANC. In considering paths with infinite continuation, branches extending from functional monomer units through bonds A → B or B → A, as well as sequences connecting two active units within a copolymer chain, are considered.

The contribution by individual active units depends on the number i of active monomer units per copolymer units A and B, i (cf. pgf $T(z)$ (eq 17)). For $i = 1$, the copolymer unit has only one bond with infinite continuation and the respective branch point does not contribute to the number of EANC (that copolymer unit is only a part of a dangling chain). None of active monomer units in a copolymer unit with $i = 2$, contribute to the number of EANC because each of them issues only two sequences with infinite continuation. Copolymer units with $i > 2$ have two end active monomer units issuing only two infinite sequences and $i - 2$ inner branch points issuing each three infinite sequences. Each inner branch point contributes to the number of EANC by $^3/_2$.

Thus, the number of EANC per component unit, N_e, is given by the equation

$$N_e = (^3/_2)\sum_{i=3}(i - 2)t_i \tag{18}$$

The sum on the right-hand side of eq 18 can be expressed in terms of the values and derivatives of pgf (eq 17). The following short-hand notation is used (p is a number usually 1 or 0):

$$T(p) \equiv T(z{=}p)$$

$$T'(p) \equiv \left(\frac{\partial T(z)}{\partial z}\right)_{z=p}$$

Because

$$T'(1) = t_1 + 2t_2 + 3t_3 + 4t_4 + ...$$

$$T(0) = t_0$$

$$T'(0) = t_1$$

$$1 = t_0 + t_1 + t_2 + t_3 + ...$$

therefore,

$$N_e = (^3/_2)[T'(1) + 2T(0) + T'(0) - 2] \tag{19}$$

The explicit expressions for the moments of the pgf $T(z)$ are as follows:

$$T(0) = n_A\frac{(1 - q_A)\zeta_{Av}}{1 - q_A\zeta_{Av}} + n_B\frac{(1 - q_B)\zeta_{Bv}}{1 - q_B\zeta_{Bv}} \tag{20}$$

$$T'(0) = n_A\frac{\xi'_A(1)}{1 - q_A\zeta_{Av}} + n_B\frac{\xi'_B(1)}{1 - q_B\zeta_{Bv}} \tag{21}$$

$$T'(1) = n_A\frac{\xi'_A(1)}{1 - q_A} + n_B\frac{\xi'_B(1)}{1 - q_B} \tag{22}$$

where

$$\xi'_A(1) = x_A\alpha_A(1 - v_B)$$

$$\xi'_B(1) = x_B\alpha_B(1 - v_A)$$

The concentration of EANC per unit volume, ν_e, a quantity determining the equilibrium modulus, is obtained from N_e

$$\nu_e = \frac{N_e\rho}{M_{0n}} \tag{23}$$

System 2—Control Hydrogels That were Synthesized via Reaction of Active Ester-Containing Precursors B with Aromatic Azo-Containing Diamines. The *control hydrogels* are obtained by cross-linking of the precursor **B** with an aromatic azo-containing diamine (component **A**) instead of a precursor **A** for the *novel hydrogels*. The pgf $F_{0n}(z_A,z_B)$ corresponding to eq 7 now reads

$$F_{0n}(z_A,z_B) = n_A(1 - \alpha_A + \alpha_A v_B)^2 + n_B\frac{(1 - q_B)\xi_B(z_A)}{(1 - q_B)\xi_B(z_A)} \tag{24}$$

Some other quantities are changed accordingly:

$$n_A = 1 - n_B = \frac{P_{Bn}x_B r_A}{2 + P_{Bn}x_B r_A}$$

$$m_A = \frac{n_A M_A}{n_A M_A + n_B P_{Bn} M_B}$$

$$M_{0n} = n_A M_A + n_B P_{Bn} M_B$$

and M_A is the molecular weight of diamine.

The pgf $F_A(z_B)$ has a simple form,

$$F_A(z_B) = 1 - \alpha_A + \alpha_A z_B \tag{25}$$

and $F_B(z_A)$ is given by eq 9. The gel-point condition equivalent to eq 11 now reads

$$(\alpha_A)_{crit} = (\alpha_B)_{crit}/r_A = \left[\frac{2q_B x_B r_A}{(1 - q_B)}\right]^{-1/2} \tag{26}$$

The extinction probabilities v_A and v_B are obtained by solution of the equations

$$v_A = 1 - \alpha_A + \alpha_A v_B \tag{27}$$

and

$$v_B = \frac{(1 - q_B)^2}{(1 - q_B\zeta_{Bv})^2} \tag{28}$$

where, as before,

$$\zeta_{Bv} = 1 - x_B + x_B(1 - \alpha_B + \alpha_B v_A)$$

The soluble and gel fractions are obtained following the same reasoning as in the case of *novel hydrogels*:

$$w_s = 1 - w_g = m_A(1 - \alpha_A + \alpha_A v_B)^2 + m_B\frac{(1 - q_B)^2\zeta_{Bw}}{(1 - q_B\zeta_{Bv})^2} \tag{29}$$

where ζ_{Bw} is defined by

$$\zeta_{Bw} = 1 - m_{XB} + m_{XB}(1 - \alpha_B + \alpha_B v_A)$$

The elastically active network chains are contributed only by component **B** because component **A** is bifunctional and does not contain any branch point. The pgf $T(z)$ now reads

$$T(z) = T(z) = n_A(\xi_A(z))^2 + n_B\frac{(1 - q_B)\xi_B(z)}{(1 - q_B\xi_B(z))} = \sum_{i=0}^{\infty} t_i z^i \tag{30}$$

where

$$\xi_A(z) = 1 - \alpha_A + \alpha_A(v_B + (1 - v_B)z)$$

$$\xi_B(z) = 1 - x_B + x_B(1 - \alpha_B + \alpha_B(v_A + (1 - v_A)z))$$

The number of EANC per component unit is given by eq 19

$$N_e = (^3/_2)[T'(1) + 2T(0) + T'(0) - 2] \tag{31}$$

The explicit expressions for the moments are now contributed only by the component **B**:

$$T(0) = n_B\frac{(1 - q_B)\zeta_{Bv}}{1 - q_B\zeta_{Bv}} \tag{32}$$

$$T'(0) = n_B\frac{\xi'_B(1)}{1 - q_B\zeta_{Bv}} \tag{33}$$

$$T'(1) = n_B\frac{\xi'_B(1)}{1 - q_B} \tag{34}$$

where

$$\xi'_B(1) = x_B\alpha_B(1 - v_A)$$

The concentration of EANC, ν_e, is given by eq 23.

Results and Discussions

Synthesis of MA-AZO-NH_2 and Its in Vitro Degradability. Although aromatic azo-bond-containing pH-sensitive hydrogels have been synthesized previously by a two-step polymer−polymer reaction,[10] synthesis based on a "one-step" polymer−polymer reaction has never been achieved. To accomplish this goal, the synthesis of an aromatic azo-bond-containing functional monomer bearing a vinyl group (for polymerization) at one end and an amino group (for reaction with active ester) at the other side was crucial.

To this end, the monomer MA-AZO-NH_2 was synthesized following the route shown in Scheme 1. The asymmetric design of the monomer ensured easy purification and possible higher stability in the synthesis process.

With respect to the aromatic azo-containing monomer, the in vitro degradability of MA-AZO-NH_2 needed to be investigated before its incorporation into hydrogels. Because of the poor water solubility of MA-AZO-NH_2 (even in the presence of small amounts of DMSO), a water-soluble copolymer, poly(HPMA-*co*-MA-AZO-NH_2) ([azo] = 3.29×10^{-4} mol/g), was synthesized as a model compound for evaluation of its in vitro degradability. Vortexing poly(HPMA-*co*-MA-AZO-NH_2) solution in the presence of sodium hydrosulfite resulted in the disappearance of color (bright yellow—typical of aromatic azo compounds) within 1 min, which demonstrated the degradability of aromatic azo bonds in a reducing enviroment. In vitro biodegradation of the aromatic azo bonds in MA-AZO-NH_2 was evaluated by incubation of poly(HPMA-*co*-MA-AZO-NH_2) with fresh rat cecum contents to monitor the disappearance of the aromatic azo bonds (Figure 1).

The generally accepted mechanism for colon degradation of aromatic azo compounds is by nonenzymatic reduction with enzyme-generated flavin molecules located in the extracellular space. The flavin molecules act as "electron shuttles" between NAD(P)H-dependent flavoprotein (the enzyme) and the aromatic azo substrate.[25,26] Any factor that affects electron transport should accelerate the degradation process.

The degradation of aromatic azo bonds in poly(HPMA-*co*-MA-AZO-NH_2) was slower compared to the degradation of methyl orange (Figure 1). Linear water-soluble copolymers containing aromatic azo bonds at the side chains were shown to form aggregates in solution with hydrophobic side chains in the core of micelles.[27] This supermolecular structure might render the electron

Scheme 1. Synthesis of *N*-Aminohexyl-4-[[4-(methacryloylamino)phenyl]azo]benzamide

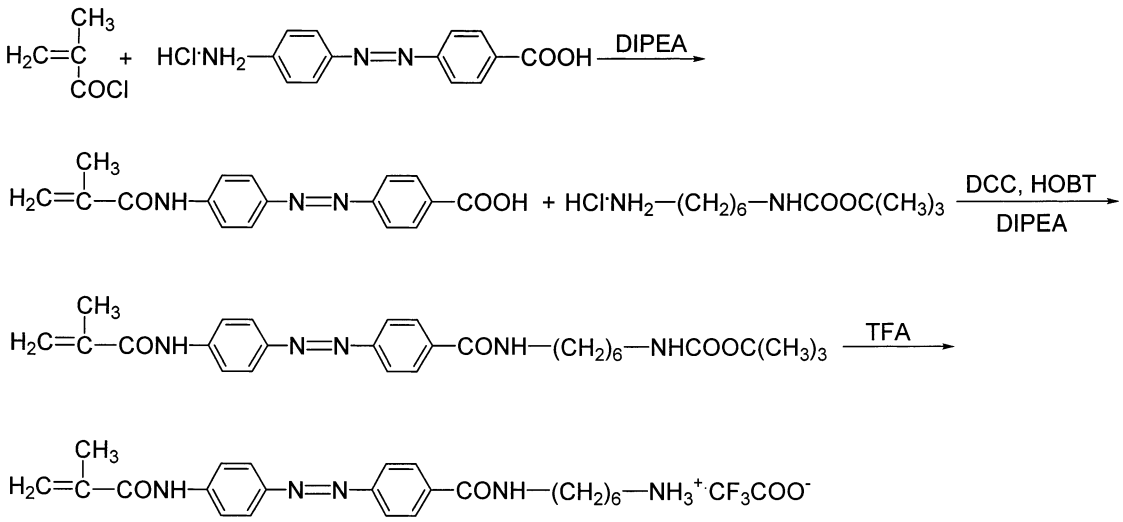

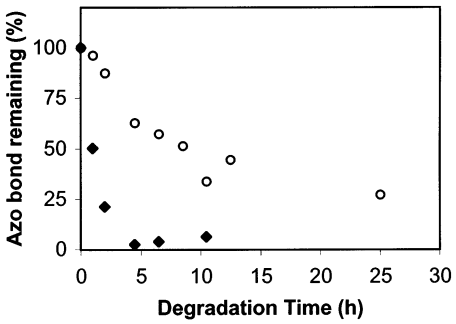

Figure 1. In vitro degradation of poly(HPMA-*co*-MA-AZO-NH_2) and methyl orange with rat cecum content: methyl orange (540 nm, ♦); poly(HPMA-*co*-MA-AZO-NH_2) (350 nm, ○). Fresh rat cecum content suspension (10 wt % in 0.1 M phosphate buffer) was preincubated with α-D-glucose at 37 °C for 14 h (anaerobic condition) followed by addition of poly(HPMA-*co*-MA-AZO-NH_2) stock solution (final concentration 1.23×10^{-4} M) or methyl orange stock solution (final concentration 5×10^{-5} M). Samples were retrieved from the degradation mixture at selected time intervals, acidified, and centrifuged. The UV absorption remaining in the supernatant was measured.

transport to aromatic azo bonds more difficult or affect its reduction potential, which would substantially decrease the degradation rate, or both. Nevertheless, about 80% of the aromatic azo bonds were degraded after 24 h of incubation. This observation supported the potential of MA-AZO-NH_2 as a building block for aromatic azo-containing cross-links in pH sensitive hydrogels for colon-specific drug delivery.

Synthesis and Characterization of Hydrogel Precursors. Polymer precursors (**A** and **B**, Scheme 2) were synthesized by free radical copolymerization. These precursors were designed on the basis of biocompatible DMAA copolymers.[28] BuAA monomer units were incorporated into the copolymer to improve the mechanical properties of the hydrogels,[29] and AA was used as a comonomer to introduce pH sensitivity. The compositions of both polymer (hydrogel) precursors are summarized in Table 1.

Previously, similar types of polymer precursors were synthesized by precipitation copolymerization in acetone.[9] However, the solubility of MA-AZO-NH_2 in acetone was found to be poor. Consequently, both precursors were polymerized in DMSO in the presence of MPA as a chain transfer agent to control their molecular weight (Table 1). The content of MA-AZO-NH_2 in precursor **A** can be easily adjusted by changing the composition of the monomer mixture. In the synthesis of precursor **B**, 6 mol % of MA-GG-ONp was always used in the copolymerization (Table 1).

Synthesis of Hydrogels by Polymer−Polymer Reaction and Their in Vitro Degradability. Novel aromatic azo-containing pH-sensitive hydrogels were synthesized by the aminolysis reaction of the active ester groups in precursor **B** with the primary amine in precursor **A**. In this reaction, there are only two possibilities: either $-NH_2$ groups react with ONp groups to form cross-links or they remain pendent. By adjusting the weight ratio of precursors **A** and **B**, hydrogels with different cross-linking densities were obtained. The weight percentage of precursors in DMSO was kept constant, and ONp groups were maintained in excess to $-NH_2$ groups.

Higher than equimolar concentrations of TFA with respect to $-NH_2$ groups in precursor **A** were needed to prevent a fast and heterogeneous gelation of the reaction mixture. Following the addition of precursor **B** solution to the precursor **A** solution, *N*-methyl morpholine (MM) was added to initiate the cross-linking reaction between ONp and NH_2 groups. In most cases, the gelation point was reached within 1 h at room temperature.

As mentioned, MA-AZO-NH_2 in the HPMA copolymer demonstrated good degradability in vitro. One may predict that MA-AZO-NH_2 in hydrogels (as a cross-linking moiety) might be degradable in simulated reductive colon condition, as well. Consequently, three hydrogels were synthesized and characterized (Table 2). Their degradability was evaluated after incubating with fresh rat cecum contents. Changes in dry weight (Figure 2), the equilibrium swelling ratio (Figure 3), and aromatic azo content (Figure 4) of the hydrogels were evaluated during the degradation process.

Because of the typical yellow color of the aromatic azo-group-containing hydrogels, the progress of degradation could be visualized by color disappearance (upon cleavage of the aromatic azo bonds). A sharp degradation front (colorless vs yellow) was observed and moved inward to the center of the gel disk as the reaction proceeded. The decolorized hydrogel became very fragile but still held its structural integrity. This could be attributed to the remaining noncleaved aromatic azo bond or possible hydrazo cross-links (aromatic azo bond

Scheme 2. Synthesis of Hydrogels by "One-Step" Polymer−Polymer Reaction

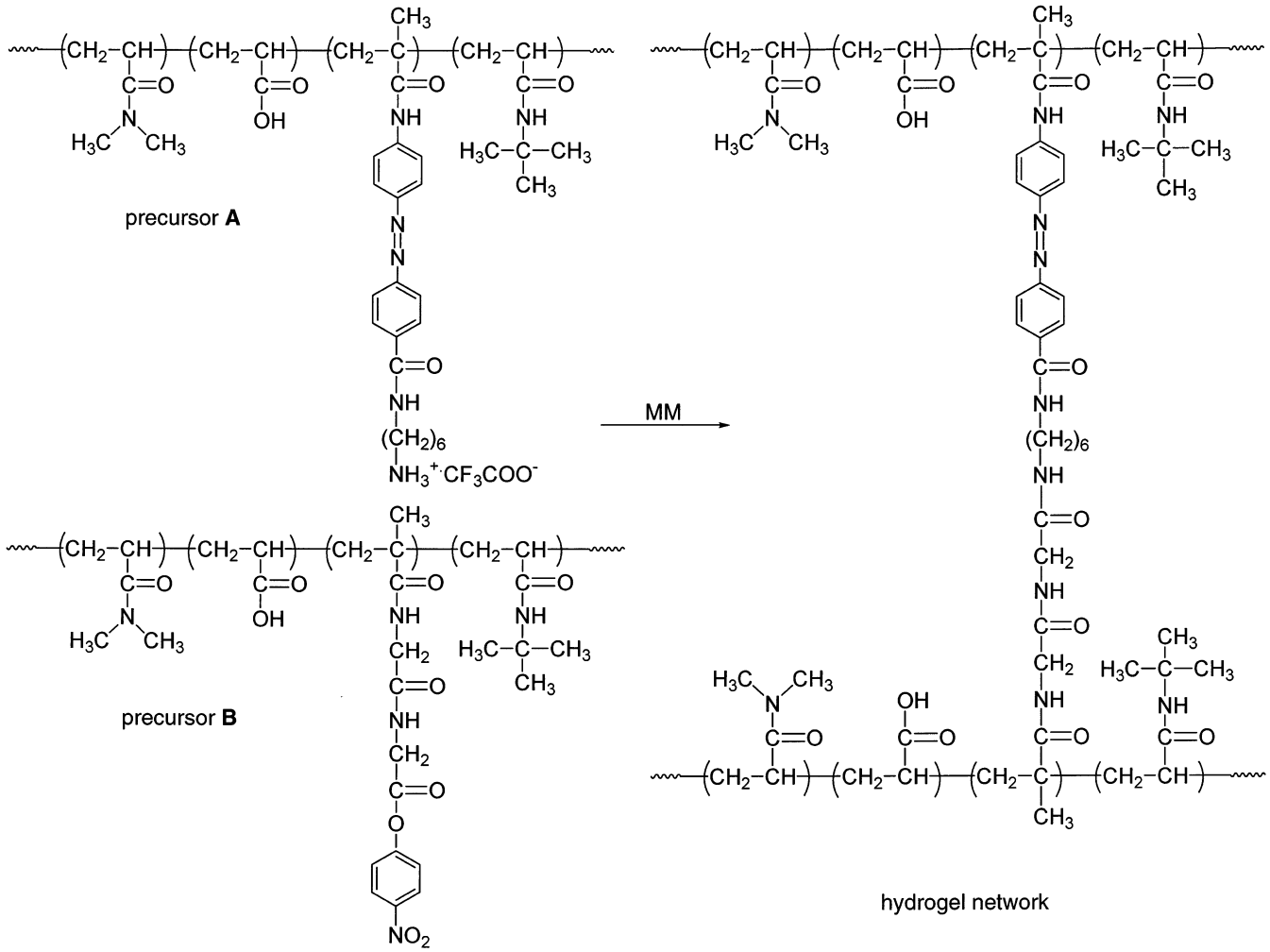

Table 1. Composition of Hydrogel Precursors

no.	BuAA (mol %)	DMAA (mol %)	AA (mol %)	MA-AZO-NH_2 (mol %)	MA-GG-ONp (mol %)	[azo][a] (mol/g)	[ONp][a] (mol/g)	M_n ($\times 10^4$)	M_w/M_n
P1-**A**	10	47	40	3		2.44×10^{-4}		1.67	1.62
P1-**B**	10	44	40		6		3.26×10^{-4}	1.69	1.47
P2-**A**	10	47	40	3		2.72×10^{-4}		1.97	1.58
P2-**B**	10	44	40		6		2.71×10^{-4}	2.35	1.48
P3-**A**	10	44	40	6		5.62×10^{-4}		3.15	2.01
P3-**B**	10	44	40		6		2.83×10^{-4}	2.92	1.62

[a] Determined spectrophotometrically.

Table 2. The Composition of Hydrogels for in Vitro Degradation Study

gels	wt %[a]	precursors **A** (wt %)[b]	precursors **B** (wt %)[b]	r_A[c]	$[azo]_{orig}$ ($\times 10^{-5}$ mol/g)	$[azo]_{measd}$[d] ($\times 10^{-5}$ mol/g)	$[NH_2]$[e] ($\times 10^{-5}$ mol/g)	Q[f]
1	15.5	P2-**A** (25.0)	P2-**B** (75.0)	2.60	6.8	7.6	0.76	42.9
2	15.5	P1-**A** (41.0)	P1-**B** (59.0)	1.93	10.0	10.0	1.50	30.8
3	15.5	P2-**A** (46.3)	P2-**B** (53.7)	1.00	12.6	12.5	2.41	26.0

[a] wt % = $[w_{precursors}/(w_{precursors} + w_{DMSO})] \times 100$. [b] (wt %) = $[w_{precursor-A}$ (or $w_{precursor-B})/(w_{precursor-A} + w_{precursor-B})] \times 100$. [c] Initial molar ratio of $[NH_2]$ to [ONp] or groups A to B. [d] Determined spectrometrically. [e] The content of NH_2 in hydrogels was determined with ninhydrin assay. [f] Swelling equilibrium ratio, $Q = w_{wet-gel}/w_{dry-gel}$.

was partially reduced into hydrazo bond, the yellow color disappeared but the cross-link was not broken).[30] This degradation pattern suggested a bulk degradation-like process, and it should be accompanied by a significant increase in the equilibrium swelling ratio and a slight loss of dry weight.[31]

The experimental data were in accordance with these predictions. The dry weight of the hydrogels decreased (Figure 2), and the equilibrium swelling ratio increased (Figure 3) during the degradation process. However, the magnitude of the increase and decrease were largely dependent on the cross-linking density (aromatic azo content) of the hydrogel. The lower the aromatic azo content in the gel was, the faster the loss of dry weight in the degradation process was, and the higher the increase in the equilibrium swelling ratio was. In the case of gel 1, which had the lowest aromatic azo content (7.6×10^{-5} mol/g), the hydrogel nearly lost all its color

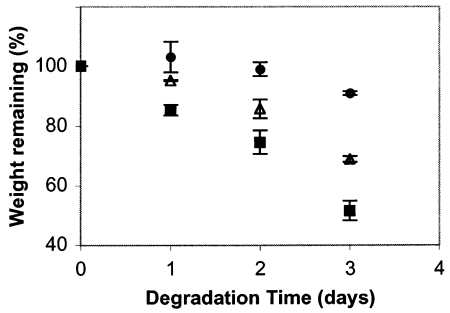

Figure 2. The changes of dry weight of hydrogels during in vitro degradation ($n = 2$): (■) gel 1; (△) gel 2; (●) gel 3. Fresh rat cecum content suspension (10 wt % in 0.1 M phosphate buffer) was preincubated with α-D-glucose at 37 °C for 14 h (anaerobic condition) followed by the introduction of hydrogels. The hydrogels were retrieved at selected time intervals, washed with ethyl alcohol/H_2O = 1/1, and gradually transferred into ethyl alcohol. The hydrogels were dried under vacuum, and their weights were measured. For composition of hydrogels, see Table 2.

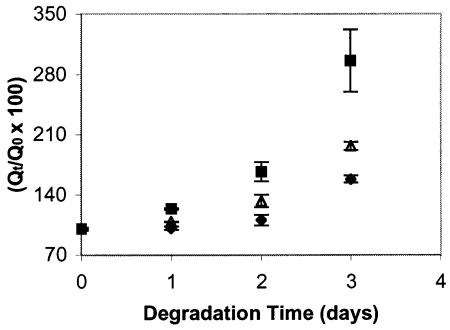

Figure 3. The changes of swelling ratio (Q_t/Q_0) of hydrogels during in vitro degradation ($n = 2$): (■) gel 1; (△) gel 2; (◆) gel 3. Fresh rat cecum content suspension (10 wt % in 0.1 M phosphate buffer) was preincubated with α-D-glucose at 37 °C for 14 h (anaerobic condition) before the start of the experiment. The degraded hydrogels were retrieved at selected time intervals, washed with ethyl alcohol/H_2O = 1/1, and gradually transferred into phosphate buffer (0.1 M). After the hydrogels were fully equilibrated in phosphate buffer, the weight of the wet gels was measured to calculate the equilibrium swelling ratio of the hydrogels. For composition of hydrogels, see Table 2.

after 3 days of degradation but held its structural integrity. It retained the highest equilibrium swelling ratio ($Q_t/Q_0 \times 100 = 296\%$, after 3 days of degradation) and lowest dry weight (52% of original weight, after 3 days of degradation). In the case of gel 3, which had the highest aromatic azo content (1.25×10^{-4} mol/g), the changes in equilibrium swelling ratio and dry weight were the lowest after 3 days of degradation ($Q_t/Q_0 \times 100 = 150\%$, 90% of original weight).

The change in hydrogel aromatic azo bond concentration vs degradation time is shown in Figure 4. The slopes correspond to the rate of bond cleavage. This information should be considered semiquantitative because of the influence of variation in azoreductase activity and relative changes in surface area of degradation front during the experiment. Nevertheless, the results permit a relative comparison between hydrogels with different aromatic azo content. Similar cleavage rates were observed in all gels. These results are in agreement with a previous report[31] and have been attributed to the presence of benzyl viologen (BV) in the degradation media. The concentration of BV was suggested to play a decisive role in hydrogel degradation. Apparently, the diffusion rate of BV in the gels studied

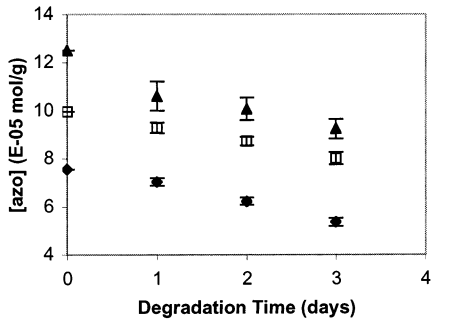

Figure 4. The changes of aromatic azo content in hydrogels during in vitro degradation ($n = 2$): (◆) gel 1; (□) gel 2; (▲) gel 3. Fresh rat cecum content suspension (10 wt % in 0.1 M phosphate buffer) was preincubated with α-D-glucose at 37 °C for 14 h (anaerobic condition) followed by the introductions of hydrogels. The degraded hydrogels were retrieved at selected time intervals, washed with ethyl alcohol/H_2O = 1/1, and gradually transferred into ethyl alcohol. The hydrogels were dried under vacuum, ground into small particles, and hydrolyzed with 2 N NaOH. After the gel was fully dissolved, the content of aromatic azo groups was determined spectrophotometrically ($\epsilon_{360nm} = 24\,160$, in 0.1 or 0.2 N NaOH). For composition of hydrogels, see Table 2.

was not dramatically different from each other. Consequently, no differences in the accessibility of the aromatic azo bonds by the BV radical cation were apparent. On the other hand, the cleavage of aromatic azo bonds of MA-AZO-NH_2 in all of the novel hydrogels was obviously much slower than those in linear poly(HPMA-*co*-MA-AZO-NH_2) (compare Figures 1 and 4). One may speculate that the presence of negative charges in these hydrogels slowed the transport of BV cation.

Predicted Structure Development and Comparison with Experimental Results. Five *novel hydrogels* (synthesized via "one-step" polymer−polymer reaction) and four *control hydrogels* (synthesized via cross-linking reaction of active ester-containing precursor **B** with aromatic azo-containing diamines) were synthesized to determine the relationship between their structure and mechanical properties. Compositions of these hydrogels are summarized in Table 3.

The gel-point conversions and the changes of structural parameters were calculated for both *control* and *novel hydrogels* using relations derived in the theoretical part of this paper. Here, it should be noted that the calculated values correspond to a ring-free system, so the differences between calculated and experimental data can be related to formation of elastically inactive cycles.

The evolution of the gel fraction, w_g, and concentration of elastically active network chains (EANC), ν_e, as a function of conversion of minority groups (amino groups, A) were calculated from different initial molar ratios of A/B (r_A) (Figure 5). The input parameters corresponded to experimental conditions (Table 3). The molar ratio of A/B groups, r_A, varied from approximately 1:1 to an excess in B (ONp component), $r_A < 1$. The dependencies have general features characteristic for cross-linking systems: an initial steep increase in w_g and an upward curvature of the increase in ν_e. Also, with increasing off-stoichiometry, the gel-point conversion increases; the soluble fraction also increases, and the concentration of EANC decreases. However, distinct differences can be observed between the *novel* and *control hydrogels*.

As can be seen in Figure 5a,b, the gel-point conversion for *novel hydrogels* is low (below 10%) and does not

Table 3. Composition of Hydrogels Synthesized via Different Methods

gels	wt %[a]	P3-**A**[b] (wt %)	P3-**B**[b] (wt %)	r_A[c]	$[azo]_{orig}$ ($\times 10^{-5}$ mol/g)	$[azo]_{measd}$[d] ($\times 10^{-5}$ mol/g)	$[NH_2]$[e] ($\times 10^{-5}$ mol/g)	Q[f]	ϕ_2^o[g]	ϕ_2[h]
4	15.54	13.4	86.6	3.27	7.5	9.2	0.97	47.4	0.141	0.0174
5	15.54	17.8	82.2	2.33	10.0	10.9	1.31	32.4	0.141	0.0254
6	15.54	22.2	77.8	1.76	12.5	11.5	1.48	24.5	0.141	0.0337
7	15.54	27.0	73.0	1.36	15.2	12.7	1.61	21.1	0.141	0.0392
8	15.54	33.0	67.0	1.02	18.5	15.4	2.43	18.1	0.141	0.0457
9	16.00		96.7	2.10	7.5	8.88	1.19	48.3	0.145	0.0170
10	16.14		95.6	1.56	10.0	11.11	0.98	31.6	0.146	0.0261
11	16.30		94.5	1.24	12.5	13.30	1.25	23.8	0.148	0.0347
12	16.45		93.5	1.03	15.0	16.10	1.32	19.5	0.149	0.0425

[a] wt % = $[w_{precursors}/(w_{precursors} + w_{DMSO})] \times 100$. [b] Gels 4−8 were synthesized with polymer−polymer reaction between precursor **A** and precursor **B**; P3-**A** or P3-**B** (wt %) = $[w_{P3-A}$ (or $w_{P3-B})/(w_{P3-A} + w_{P3-B})] \times 100$; Gels 9−12 were synthesized with the reaction of P3-**B** with *N*,*N*′-(ω-aminocaproyl)-4,4′-diaminoazobenzene; P3-**B** (wt %) = $[w_{P3-B}/(w_{diamine} + w_{P3-B})] \times 100$; All precursors have been described in Table 1. [c] Initial molar ratio of $[NH_2]$ to [ONp] or groups A to B. [d] The aromatic azo content in hydrogels was determined spectrometrically. [e] The content of NH_2 in hydrogels was determined with ninhydrin assay. [f] Swelling equilibrium ratio, $Q = w_{wet-gel}/w_{dry-gel}$. [g] Volume fraction of polymer precursors at network formation, $\phi_2^o = (w_p/d_p)/(w_p/d_p + w_{DMSO}/d_{DMSO})$. [h] Volume fraction of the polymer precursors in the swollen hydrogel, $\phi_2 = (w_p/d_p)/(w_p/d_p + w_{H_2O}/d_{H_2O})$.

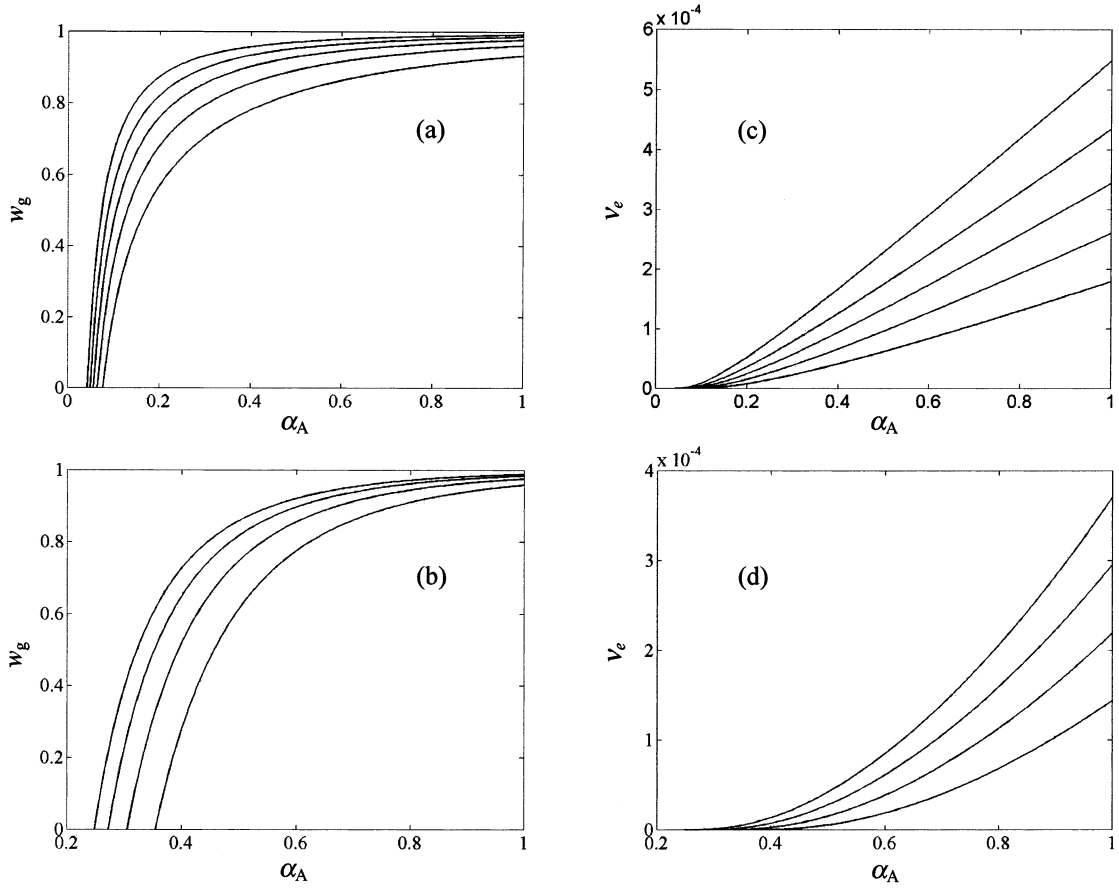

Figure 5. Panel a shows the calculated dependence of the gel fraction (w_g) on conversion of amino groups, α_A, for *novel hydrogels*. Molar ratio of [ONp]/$[NH_2]$ ($1/r_A$) = 3.27, 2.33, 1.76, 1.36, and 1.02 (gels 4−8 in Table 4) from bottom to top. Panel b shows the calculated dependence of the gel fraction (w_g) on conversion of amino groups, α_A, for *control hydrogels*. Molar ratio of [ONp]/$[NH_2]$ ($1/r_A$) = 2.10, 1.56, 1.24, and 1.03 (gels 9−12 in Table 4) from bottom to top. Panel c shows the calculated dependence of the concentration of EANC, ν_e [mol/cm^3], on conversion of amine groups, α_A, for *novel hydrogels*. Molar ratio of [ONp]/$[NH_2]$ ($1/r_A$) = 3.27, 2.33, 1.76, 1.36, and 1.02 (gels 4−8 in Table 4) from bottom to top. Panel d shows the calculated dependence of the concentration of EANC, ν_e [mol/cm^3], on conversion of amine groups, α_A, for *control hydrogels*. Molar ratio of [ONp]/$[NH_2]$ ($1/r_A$) = 2.10, 1.56, 1.24, and 1.03 (gels 9−12 in Table 4) from bottom to top.

increase too much with increasing off-stoichiometry. However, in the case of *control hydrogels*, the gel-point conversions are higher by a factor of 4−5 and the effect of off-stoichiometry is larger when compared to the *novel hydrogels*. Indeed, as observed in experiments, the gelation of *novel hydrogels* could be observed in 10 min, while it took a considerably longer time for the *control hydrogels* to gel.

The calculated dependencies shown in Figure 5a,b indicate that the increase in the weight of the gel is much steeper for the polymer−polymer system. It can also be seen that some soluble fraction always remains at 100% conversion for both types of hydrogels. This is in good agreement with the experimental fact that 5−10% of dry weight loss was usually observed after purification of both types of hydrogels, which was

Table 4. The Characteristics (Determined Experimentally and Calculated Theoretically) of Hydrogels Synthesized via Different Methods

gels	r_A[a]	α_A(exptl)[b]	w_g(calcd)[c]	$\nu_e \times 10^4$ (mol/cm^3) calcd[d]	$\nu_e \times 10^4$ (mol/cm^3) exptl[e]	$\alpha_{A,inter}$(calcd)[f]	$\Delta\alpha_{A,cycl}$[g]
4	3.27	0.895	0.920	1.53	0.264	0.323	0.572
5	2.33	0.880	0.952	2.19	0.86	0.469	0.411
6	1.76	0.871	0.970	2.88	1.59	0.564	0.307
7	1.36	0.873	0.981	3.67	2.08	0.565	0.308
8	1.02	0.842	0.988	4.45	2.80	0.581	0.261
9	2.10	0.933	0.947	1.15	0.43	0.741	0.233
10	1.56	0.956	0.971	1.94	1.16	0.808	0.163
11	1.24	0.953	0.981	2.60	2.35	0.916	0.065
12	1.03	0.959	0.987	3.33	3.32	0.957	0.002

[a] Initial molar ratio of [NH_2] to [ONp] or groups A to B. [b] Molar conversions of A or NH_2 group determined experimentally. [c] Calculated gel weight fraction. [d] The calculated concentration of elastically active network chains (EANC). [e] The experimentally determined concentration of elastically active network chains (EANC). [f] The conversion of A (amino group) that formed bonds that were effective in the formation of EANC but not those engaged in formation of elastically inactive cycles was also calculated from the experimental value of ν_e. [g] $\Delta\alpha_{A,cycl}$ (α_A(exptl) − $\alpha_{A,inter}$(calcd)) shows the amount of reacted A (amino group) involved in the formation of elastically inactive cycles.

apparently due to the removal of the soluble fraction.

With the increase in conversion of minority groups (amino groups, α_A), the concentration of EANC, ν_e, in the *novel hydrogels* builds up faster than that in *control hydrogels* (Figure 5c,d). Furthermore, the final concentration of EANC in the *novel hydrogels* is also higher and less-sensitive to increasing off-stoichiometry when compared to the *control hydrogels*.

These differences may be explained by a low functionality of diamine used in *control hydrogels* compared to the precursor **A** in *novel hydrogels*. However, the degree of polymerization and compositional distributions of the polymeric precursors in the case of the *novel hydrogels* are operative as well.

The value of the gel-point conversion is determined by the second moment of functionality distribution, and this results both from the degree of polymerization and from compositional distributions. This is the reason that the gel point conversion is considerably lower in the case of *novel hydrogels*. The compositional distributions of both polymeric precursors give rise to the residual sol fraction at 100% conversion. The differences between the two systems are even more distinct if one plots ν_e as a function of the molar ratio r_A (data not shown).

The model used in these calculation has a few assumptions. Among them, the presumed absence of *intramolecular* reactions that lead to the formation of cyclization needs to be reconsidered. In fact, a comparison between the calculated values and experimental results in Table 4 shows that indeed cyclization is not negligible. Experimentally, the concentration of EANC, ν_e, was determined from the equilibrium compression modulus of swollen hydrogels and calculated according to eq 2. The theoretical values of ν_e were calculated, and their values can be seen in Figure 5c,d.

The conversion of A (amino) groups to intermolecular bonds ($\alpha_{A,inter}$ calcd) was calculated from the experimental values of ν_e using the calculated dependences of ν_e on α_A. It corresponds to conversion of amino groups into bonds that are effective in the formation of EANC but not those engaged in the formation of elastically inactive cycles. Therefore, the difference between the experimental conversion and the value calculated from equilibrium modulus represents the fraction of bonds lost in elastically inactive cycles.

From the experimental and calculated data in Table 4, one can observe that the final conversions of the minority groups (amino group, A) are lower in the case of *novel hydrogels*. This may reflect the different diffusion rates of the low molecular weight diamine and the primary amino groups at side chain termini of precursor **A** during the formation of the hydrogel networks. The reduced frequency of collisions between polymer-bound primary amino and ONp groups might ultimately result in fewer conversions of the amino groups in the *novel hydrogels* than those in the *control hydrogel*.

Compared with results of networks from telechelic precursors reported previously,[11] cyclization in both types of hydrogels discussed here was higher. Several factors may account for this. However, different flexibilities of the copolymer chains and cross-linking in the presence of diluent seem to be the main factors.

In Table 4, $\Delta\alpha_{A,cycl}$ (α_A(exptl)) − $\alpha_{A,inter}$(calcd)) shows the amount of reacted A (amino group) involved in the formation of elastically inactive cycles. Apparently, the extent of cyclization is higher in the case of *novel hydrogels* compared to the *control hydrogels*. In fact, the experimentally determined conversion of minority group (amino group, α_A(exptl)) for one of the *control hydrogels* (a stoichiometric system, gel 12 in Table 4) is almost the same as the calculated result ($\alpha_{A,inter}$(calcd)), that is, cyclization is negligible. This phenomenon might be attributed to the rigidity of the aromatic azo-containing diamine used in the synthesis of *control hydrogels*, compared to the more flexible precursors **A** (containing amino group) in the *novel hydrogels* synthesis.

The fraction of bonds wasted in cycles increased when the excess of ONp groups (precursor **B**) was enlarged, and the system was closer to the gel point (Table 4). This is possibly due to a dilution of the reacting systems by excess of precursor **B**. This excess affects the *intermolecular* reaction but not the *intramolecular* one, particularly that involving neighboring groups on copolymer chains. In addition, larger cyclic structures may be elastically inactive at low cross-linking densities. These large ring structures become a part of the network when cross-linking proceeds (activation of EIC[11]). However, to elucidate the competition between *inter-* and *intramolecular* reactions and formation of elastically inactive cycles in more detail, further studies are necessary, such as the effect of off-stoichiometry and dilution on the shift of the gel-point conversion and changes of molecular weight averages before the gel point.

Conclusions

(1) *N*-(1-Aminohexyl)-4-[[4-(methacryloylamino)phenyl]azo]benzamide (MA-AZO-NH_2) was synthesized and copolymerized with BuAA, DMAA, and AA. The resulting polymer precursor **A** enabled the synthesis of novel aromatic azo-containing pH-sensitive hydrogels by a "one-step" polymer−polymer reaction. *Control hydrogels* were synthesized by cross-linking polymer precursor **B** with low molecular weight diamine.

(2) The *novel hydrogels* were degradable when incubated in rat cecum contents. The process of hydrogel degradation (changes in dry weight and *Q*) was largely dependent on the cross-linking density of the hydrogels. However, for hydrogels with different cross-linking densities, similar aromatic azo cleavage rates were achieved with benzyl viologen as an electron mediator.

(3) The development of the network structure of the hydrogels was described by the statistical theory of branching processes. In the *novel hydrogels*, the conversion of amino groups is lower and the concentration of elastically active network chains is built up faster than those in the *control hydrogels* (in which the amine-containing copolymer is replaced by a low molecular weight diamine). Comparison of experimental and calculated concentrations of EANC revealed that approximately 60% of the bonds are lost in elastically inactive cycles formed. The loss of bonds in EIC is more significant in the case of the *novel hydrogels*, in which the polymer−polymer reactions offer a higher probability for ring closing.

Acknowledgment. This research was supported in part by NIH Grant EB00251. We also acknowledge the funding for NMR instrumentation provided by NIH Grant RR14768. M.D. and K.D. acknowledge the support provided by Grant Agency of the Czech Republic (Grant 203/99/D062).

Note Added After ASAP Posting

This article was released ASAP on 08/30/2002 with errors on page 7793, right-hand column, paragrah 2, and on page 7797, right-hand column, paragraph 3. The correct version was posted on 09/24/2002.

References and Notes

(1) Saffran, M.; Kumar, S. G.; Savariar, C.; Burnham, J. C.; William, F.; Neckers, D. C. *Science* **1986**, 1081.
(2) Kopeček, J.; Kopečková, P. In *Oral Colon-Specific Drug Delivery*; Friend, D. R., Ed.; CRC Press: Boca Raton, FL, 1992; pp 189−221.
(3) Rubinstein, A.; Tirosh, B.; Baluom, M.; Nassar, T.; David, A.; Radai, R.; Gliko-Kabir, I.; Friedman, M. *J. Controlled Release* **1997**, *46*, 59.
(4) Leopold, C. S. *Pharm. Sci. Technol. Today* **1999**, *2* (5), 197.
(5) Akala, E. O.; Kopečková, P.; Kopeček, J. *Biomaterials* **1998**, *19*, 1037.
(6) Samyn, C.; Kalala, W.; Van den Mooter, G.; Kinget, R. *Int. J. Pharm.* **1995**, *121*, 211.
(7) Yamaoka, T.; Makita, Y.; Sasatani, H.; Kim, S.-I.; Kimura, Y. *J. Controlled Release* **2000**, *66*, 187.
(8) Kakoulides, E. P.; Smart, J. D.; Tsibouklis, J. *J. Controlled Release* **1998**, *52*, 291.
(9) Yeh, P.-Y.; Kopečková, P.; Kopeček, J. *J. Polym. Sci., Part A: Polym. Chem.* **1994**, *32*, 1627.
(10) Ghandehari, H.; Yeh, P.-Y.; Kopečková, P.; Kopeček, J. *Macromol. Chem. Phys.* **1996**, *197*, 965.
(11) Dušek, K. In *Telechelic Polymers: Synthesis and Application*; Goethals, E. J., Ed.; CRC Press: Boca Raton, FL, 1989; p 89.
(12) Dušek, K.; Dušková-Smrčková, M. *Prog. Polym. Sci.* **2000**, *25*, 1215.
(13) Dušek, K.; Šomvárský, J. *Polym. Int.* **1997**, *44*, 225.
(14) Dušek, K. *Network Formation, in Processing of Polymers*; Materials Science and Technology, Vol. 18; Verlag Chemie: Weinheim, Germany, 1997; p 401.
(15) Morishima, Y.; Tsuji, M.; Seki, M.; Kamachi, M. *Macromolecules* **1993**, *26*, 3299.
(16) Kopeček, J.; Bažilová, H. *Eur. Polym. J.* **1973**, *9*, 7.
(17) Rejmanová, P.; Labský, L.; Kopeček, J. *Macromol. Chem.* **1977**, *178*, 2159.
(18) Report of the AVMA Panel on Euthanasia. *J. Am. Vet. Med. Assoc.* **2001**, *218*, 679.
(19) Lu, Z.-R.; Gao, S.-Q.; Kopečková, P.; Kopeček, J. *Bioconjugate Chem.* **2000**, *11*, 3.
(20) Moore, S.; Stein, W. H. *J. Biol. Chem.* **1954**, *211*, 907.
(21) Cluff, E. F.; Gladding, E. K.; Pariser, R. A. *J. Polym. Sci.* **1960**, *45*, 341.
(22) Ulbrich, K.; Ilavský, M.; Dušek, K.; Kopeček, J. *Eur. Polym. J.* **1977**, *13*, 579.
(23) Flory, P. J. *Polymer* **1979**, *20*, 1317.
(24) Flory, P. J. *Principles of Polymer Chemistry*; Cornell University Press: Ithaca, NY, 1951; p 319.
(25) Walker, R.; Gingell, R.; Murrells, D. F. *Xenobiotica* **1971**, *1*, 221.
(26) Gingell, R.; Walker, R. *Xenobiotica* **1971**, *1*, 231.
(27) Koňák, Č.; Kopečková, P.; Kopeček, J. *Macromolecules* **1992**, *25*, 5451.
(28) Kopeček, J.; Šprincl, L.; Bažilová, H.; Vacík, J. *J. Biomed. Mater. Res.* **1973**, *7*, 111.
(29) Ulbrich, K., Kopeček, J. *J. Polym. Sci., Polym. Symp.* **1979**, *66*, 209.
(30) Kimura, Y.; Makita, Y.; Kumagai, T.; Yamane, H.; Kitao, T.; Sasatani, H.; Kim, S. I. *Polymer* **1992**, *33*, 5294.
(31) Yeh, P.-Y.; Kopečková, P.; Kopeček, J. *Macromol. Chem. Phys.* **1995**, *196*, 2183.

MA020745K